Bukti korespondensi

Submission no: JMRT_2018_825
Submission title: Sugar palm (Arenga pinnata (Wurmb.) Merr) cellulosic fibre hierarchy: A comprehensive approach from macro to nano scale
Corresponding author: Professor S.M. Sapuan

Track your co-authored submission to Journal of Materials Research and Technology ▶ Kotak Masuk ×

Journal of Materials Research and Technology <EviseSupport@elsevier.com>
kepada saya ▾

21 Feb 2019, 09.18

Inggris ▾ > Indonesia ▾ Terjemahkan pesan

Nonaktifkan untuk: Inggris ×

Dear Dr syafri,

Submission no: JMRT_2018_825
Submission title: Sugar palm (Arenga pinnata (Wurmb.) Merr) cellulosic fibre hierarchy: A comprehensive approach from macro to nano scale
Corresponding author: Professor S.M. Sapuan
Listed co-author(s): Dr Mohd Adrinata Shaharuzaman, Dr Noor Azammi Abdul Murat, Dr Mohamad Ridzwan Ishak, Professor Hairul Abral, Dr M.N.F. Norrrahim, Dr N. Mohd Nurazzi, Mr. R.A. Ilyas, Dr Nasmi Herlina Sari, Dr edi syafri, Dr Ridhwan Jumaidin, Mr A.M. Radzi, Dr Mochamad Asrofi, Dr Rushdan Ibrahim, Mr M.R.M. Huzaifah, Mrs Atikah Mahamud, Dr. E. S. Zainudin

Professor Sapuan has submitted a manuscript to Journal of Materials Research and Technology and listed you as a co-author. This email is to let you know we will be in contact with updates at each decision stage of the submission process.

The link below takes you to a webpage where you can sign in to our submission system using your existing Elsevier profile credentials or register to create a new profile. You will then have the opportunity to tailor these updates and view reviewer and editor comments once they become available.

http://www.evise.com/profile/api/navigate/JMRT?resourceUrl=%2Fco-author%2F%3Fdgcid%3Dinvite_email_coauthoroutreach22387854%23%2FJMRT%2Fsubmission%2FJMRT_2018_825

If you are not a co-author of this manuscript, please contact Researcher Support at: https://service.elsevier.com

Thank you very much for your submission and we will be in touch as soon as we have any news to share.

Journal of Materials Research and Technology

If you do not wish to receive further update emails on your co-authored submission, you can unsubscribe via this link:

Manuscript Details

Manuscript number	JMRT_2018_825_R4
Title	Sugar palm (Arenga pinnata (Wurmb.) Merr) cellulosic fibre hierarchy: A comprehensive approach from macro to nano scale
Short title	Sugar palm (Arenga pinnata (Wurmb.) Merr) cellulosic fibre hierarchy: A comprehensive approach from macro to nano scale
Article type	Original article

Abstract

Sugar palm (Arenga pinnata) fibre is considered as a waste product of the agricultural industry. This paper is investigating the isolation of nanofibrillated cellulose from sugar palm fibres produced by a chemo-mechanical approach, thus opening a new way to utilize waste products more efficiently. Chemical pre-treatments, namely delignification and mercerization processes, were initially involved to extract the sugar palm cellulose. Then, mechanical pre-treatment was performed by passing the sugar palm cellulose through a refiner to avoid clogging in thesubsequent process of high pressurized homogenization. Nanofibrillated cellulose was then characterized by its chemical properties (Fourier Transform Infrared spectroscopy), physical morphological properties (i.e. scanning electron microscopy, transmission electron microscopy, X-ray diffraction analysis), and thermogravimetric analysis.

The nanofibres were attained at 500 bar for 15 cycles with 92% yield. The results showed that the average diameter and length of the nanofibrillated cellulose were found to be 5.5±0.99nm and several micrometres, respectively. They also displayed higher crystallinity (81.2%) and thermal stability compared to raw fibres, which served its purpose as aneffective reinforcing material for use as bio-nanocomposites. The nanocellulose developed promises to be a very versatile material by having a huge potential in many applications, encompassing bio-packaging to scaffolds for tissue regeneration.

Keywords	Agricultural waste; sugar palm fibre; nanocellulose; sugar palm nanofibrillated cellulose; high pressurize homogenization (HPH)
Taxonomy	Disposal, Microstructure Characterization, Materials Testing, Mineral Extraction
Corresponding Author	S.M. Sapuan
Corresponding Author's Institution	Universiti Putra Malaysia
Order of Authors	R.A. Ilyas, S.M. Sapuan, Mohamad Ridzwan Ishak, E. S. Zainudin, Rushdan Ibrahim, Hairul Abral, Mochamad Asrofi, Atikah Mahamud, M.R.M. Huzaifah, A.M. Radzi, Noor Azammi Abdul Murat, Mohd Adrinata Shaharuzaman, N. MohdNurazzi, edi syafri, Nasmi Herlina Sari, M.N.F. Norrrahim, Ridhwan Jumaidin
Suggested reviewers	Salim Hiziroglu

Submission Files Included in this PDF

File Name [File Type]

4th Detailed Responses to the editors and reviewers.docx [Response to Reviewers]Highlights.docx

[Highlights]

Graphical Abstract.docx [Graphical Abstract]

4th Revised Main Manuscript.docx [Manuscript File]Figures.docx

[Figure]

Tables.docx   [Table] Author_Agreement.docx

[Author Agreement]

To view all the submission files, including those not included in the PDF, click on the manuscript title on your EVISE Homepage, then click 'Download zip file'.

Research Data Related to this Submission

There are no linked research data sets for this submission. The following reason is given:Data will be made available on request

Comments from the editor and reviewer:

-Editor

 - L 55: Please, use either "5.50 ± 0.99 nm" or "5.5 ± 1.0 nm" (same in Ls 346 and 357)

Dear editor and reviewer, thanks for the comment. The comment from the editor and reviewer had been carefully revised in the revised manuscript. The font color of revisedword had changed to red color to facilitate the editor and reviewer to see the correctionthat had been made.

 - L 85: Please, delete the comma in all citations such as "Khalil et al. [8]"

Dear editor and reviewer, thanks for the comment. The comment from the editor andreviewer had been carefully revised in the revised manuscript.

 - L 190: Please, use "Eq.(1)" and similar for other Equations along the text

Dear editor and reviewer, thanks for the comment. The comment from the editor and reviewer had been carefully revised in the revised manuscript. The font color of revisedword had changed to red color to facilitate the editor and reviewer to see the correctionthat had been made.

 - Ls 224, 234 and 236: Please indicate the greek letter corresponding to "viscosity" since the image is not clear.

Dear editor and reviewer, thanks for the comment. The comment from the editor andreviewer had been carefully revised in the revised manuscript. The greek letter corresponding to "viscosity" is [η].

 - L 306: ". 3.93 ± 0.26 um"

Dear editor and reviewer, thanks for the comment. The comment from the editor and reviewer had been carefully revised in the revised manuscript. The font color of revisedword had changed to red color to facilitate the editor and reviewer to see the correctionthat had been made.

 - Ls 347 and 351: Please, use either "9 ± 2 nm" or "9.00 ± 1.89 nm"

Dear editor and reviewer, thanks for the comment. The comment from the editor and reviewer had been carefully revised in the revised manuscript. The font color of revisedword had changed to red color to facilitate the editor and reviewer to see the correctionthat had been made.

- L 378: " (8.36 ± 0.10 %) ..(12.86 ± 0.89 %) "

Dear editor and reviewer, thanks for the comment. The comment from the editor and reviewer had been carefully revised in the revised manuscript. The font color of revisedword had changed to red color to facilitate the editor and reviewer to see the correctionthat had been made.

  - L 381: "...to have abundant formations..."

Dear editor and reviewer, thanks for the comment. The comment from the editor and reviewer had been carefully revised in the revised manuscript. The font color of revisedword had changed to red color to facilitate the editor and reviewer to see the correctionthat had been made.

  - L 383: "...led to fibres swell and to become..."

Dear editor and reviewer, thanks for the comment. The comment from the editor and reviewer had been carefully revised in the revised manuscript. The font color of revisedword had changed to red color to facilitate the editor and reviewer to see the correctionthat had been made.

  - L 404: "...2,963.33..."

Dear editor and reviewer, thanks for the comment. The comment from the editor and reviewer had been carefully revised in the revised manuscript. The font color of revisedword had changed to red color to facilitate the editor and reviewer to see the correctionthat had been made.

  - L 407: "...(2,963.33)..."

Dear editor and reviewer, thanks for the comment. The comment from the editor and reviewer had been carefully revised in the revised manuscript. The font color of revisedword had changed to red color to facilitate the editor and reviewer to see the correctionthat had been made.

  - L 405: "...in the XRD patterns. "

Dear editor and reviewer, thanks for the comment. The comment from the editor and reviewer had been carefully revised in the revised manuscript. The font color of revisedword had changed to red color to facilitate the editor and reviewer to see the correctionthat had been made.

  - L 456: "...arranged into crystalline..."

Dear editor and reviewer, thanks for the comment. The comment from the editor and reviewer had been carefully revised in the revised manuscript. The font color of revisedword had changed to red color to facilitate the editor and reviewer to see the correctionthat had been made.

-Reviewer 4

   - Although most of the previous comments have been appropriately responded and accordingly the manuscript is modified, the authors have not replied to the word 'Surprisingly' (Line No. 449 on page 11). This should have been replied to for the benefit of the readers of this paper when published.
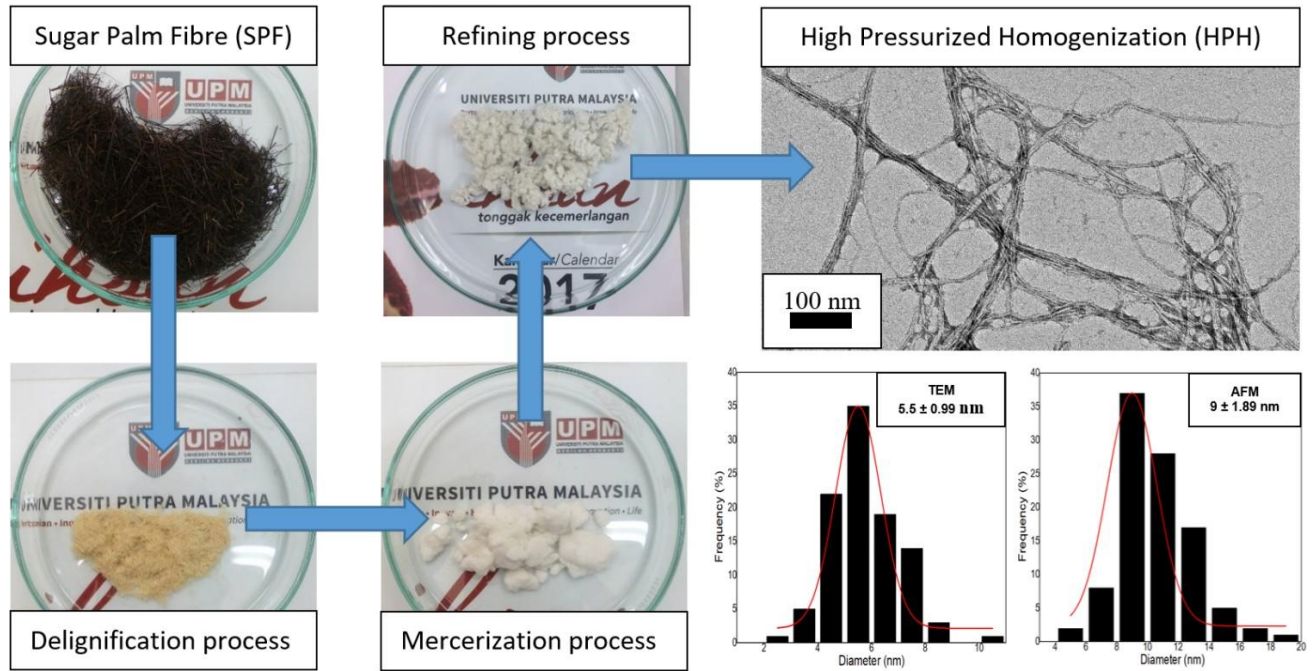
Dear reviewer, thanks for the comments. The word surprising had been removed toavoid confusion.

Dear editor and reviewer, thanks for positive comments. Hopefully this manuscript can be published in Journal of Materials Research and Technology.

Highlights:

- Sugar palm nanofibrillated cellulose (SPNFCs) was isolated from sugar palm fibres.

- Chemo-mechanical method was used to obtain SPNFCs.

- TEM, FESEM and AFM micrograph showed the thread-shape and nano-size of SPNFCs.

- TGA and XRD analysis showed improvement in thermal and crystallinity of SPNFCs.

Graphical Abstract

Sugar Palm Fibre (SPF) — Refining process — High Pressurized Homogenization (HPH)

100 nm

TEM
5.5 ± 0.99 nm

AFM
9 ± 1.89 nm

Delignification process — Mercerization process

1 **Sugar palm (*Arenga pinnata (Wurmb.*) *Merr*) cellulosic fibre hierarchy: A**
2 **comprehensive approach from macro to nano scale**

3 **R.A. Ilyas[a,b*], S.M. Sapuan[a,b,c*], Rushdan Ibrahim[d], Hairul Abral[e], M.R. Ishak[f], E.S.**
4 **Zainudin[a], Mochamad Asrofi[g], M.S.N. Atikah[h], M.R.M. Huzaifah[a], A.M. Radzi[a,i], A.M.**
5 **Noor Azammi[b,j], M.A. Shaharuzaman[b,k,l], N. Mohd Nurazzi[a,b], Edi Syafri[m], Nasmi**
6 **Herlina Sari[n], M.N.F. Norrrahim[o], R. Jumaidin[p]**

7

8 [a]Laboratory of Biocomposite Technology, Institute of Tropical Forestry and Forest
9 Products, Universiti Putra Malaysia, 43400 UPM Serdang, Selangor, Malaysia
10 [b]Department of Mechanical and Manufacturing Engineering, Universiti Putra Malaysia,
11 43400 UPM Serdang, Selangor, Malaysia
12 [c]Advanced Engineering Materials and Composites Research Centre, Department of
13 Mechanical and Manufacturing Engineering, Universiti Putra Malaysia, 43400 UPM
14 Serdang, Selangor, Malaysia
15 [d]Pulp and Paper Branch, Forest Research Institute Malaysia, 52109 Kepong, Selangor,
16 Malaysia
17 [e]Department of Mechanical Engineering, Andalas University, 25163 Padang, Sumatera
18 Barat, Indonesia
19 [f]Department of Aerospace Engineering, Universiti Putra Malaysia, 43400 UPM Serdang,
20 Selangor, Malaysia
21 [g]Laboratory of Material Testing, Department of Mechanical Engineering, University of
22 Jember, Kampus Tegalboto, Jember 68121, East Java, Indonesia
23 [h]Department of Chemical and Environmental Engineering, Universiti Putra Malaysia,
24 43400 UPM Serdang, Selangor, Malaysia
25 [i]Faculty of Engineering and Technology, Linton Unversity Colledge, 71700 Mantin,
26 Negeri Sembilan, Malaysia
27 [j]Automotive Department, Malaysia France Institute, University Kuala Lumpur, 43650,
28 Bandar Baru Bangi, Selangor, Malaysia
29 [k]Faculty of Mechanical Engineering, Universiti Teknikal Malaysia Melaka, Hang Tuah
30 Jaya, 76100 Durian Tunggal, Melaka, Malaysia
31 [l]Centre for Advanced Research on Energy, Universiti Teknikal Malaysia Melaka, Hang
32 Tuah Jaya, 76100 Durian Tunggal, Melaka, Malaysia
33 [m]Department of Agricultural Technology, Politeknik Pertanian, Payakumbuh, Indonesia
34 [n]Mataram University, Jalan Majapahit No.2 Mataram, West Nusa Tenggara Indonesia
35 [o]Research Center for Chemical Defence (CHEMDEF), University Pertahanan Nasional
36 Malaysia, Kem Perdana Sungai Besi, 57000, Kuala Lumpur, Malaysia
37 [p]Fakulti Teknologi Kejuruteraan Mekanikal dan Pembuatan, Universiti Teknikal Malaysia
38 Melaka, Hang Tuah Jaya, 76100 Durian Tunggal, Melaka, Malaysia

39 * Corresponding author. Tel.: +603-89471788; Fax: +603-86567122

40 E-mail address: sapuan@upm.edu.my; ahmadilyasrushdan@yahoo.com

41

42 **ABSTRACT**

43   Sugar palm (*Arenga pinnata*) fibre is considered as a waste product of the agricultural

44   industry. This paper is investigating the isolation of nanofibrillated cellulose from sugar

palm fibres produced by a chemo-mechanical approach, thus opening a new way to utilize waste products more efficiently. Chemical pre-treatments, namely delignification and mercerization processes, were initially involved to extract the sugar palm cellulose. Then, mechanical pre-treatment was performed by passing the sugar palm cellulose through a refiner to avoid clogging in the subsequent process of high pressurized homogenization. Nanofibrillated cellulose was then characterized by its chemical properties (Fourier Transform Infrared spectroscopy), physical morphological properties (i.e. scanning electron microscopy, transmission electron microscopy, X-ray diffraction analysis), and thermogravimetric analysis. The nanofibres were attained at 500 bar for 15 cycles with 92% yield. The results showed that the average diameter and length of the nanofibrillated cellulose were found to be 5.5 ± 1.0 nm and several micrometres, respectively. They also displayed higher crystallinity (81.2%) and thermal stability compared to raw fibres, which served its purpose as an effective reinforcing material for use as bio-nanocomposites. The nanocellulose developed promises to be a very versatile material by having a huge potential in many applications, encompassing bio-packaging to scaffolds for tissue regeneration.

1. Introduction

Lignocellulosic nanomaterials have attracted interest from researchers as the alternative materials to replace synthetic materials, due to their sustainability and abundant source [1–3]. Nanofibrillated cellulose (NFC) from plant lignocellulose has particularly huge potential in many applications, from flexible food biodegradable packaging to scaffolds for tissue regeneration [1,4–7]. Nevertheless, the effectiveness of NFC production is still challenging with respect to commercial scale, high capacity, and energy consumption. Therefore, despite several methods for producing NFC that have been described by Khalil et al. [8] it is recently reported that all cellulosic fibre preparations involve some types of enzymatic or chemical pre-treatments prior to intensive mechanical disintegration. These enzymatic and chemical pre-treatments have been conducted to facilitate the disintegration of cellulose into nanofibrils, thus reducing the energy consumption. To date, several types of mechanical disintegration methods have been used to produce nanofibrillated cellulose, including high pressurized homogenization (HPH), microfluidization, ultrafine grinding or refining, cryocrushing in liquid nitrogen, high intensity ultrasonication (HIUS), and high speed blending [8–10]. HPH process includes passing cellulose slurry at a high pressure into a vessel through a very small nozzle. The fibres are then exposed to a large pressure drop with impact and shearing forces, as this valve opens and closes in rapid succession. The combination of impact and shearing forces promotes a high degree of nanofibrillation of the cellulose fibres, resulting in NFC [11]. According to Khalil et al. [8] HPH can be considered as an efficient method for refining of cellulosic fibres due to its simplicity, high efficiency, and non-requirement for organic solvents.

In the past decades, a wide range of agro-industrial residues had been used as the sources of NFC preparation, such as potato tuber cells [12], cassava bagasse [13], sugarcane bagasse, banana peels [14], wheat straw [15], rice straw [16], coir fibre [17], sugar beet [18], corn husk, and oat hulls [19]. In tropical countries, sugar palm fibres are presently categorised as waste products from sugar palm cultivation, whereby sugar palm is a multipurpose plant grown in these countries. The plant is a member of the *Palmae* family having almost 181 genera and an estimated number of 2600 species known globally. The fibres are mainly lignocellulosic and multicellular, which are found to have a high percentage of cellulose content [20-22]. Therefore, sugar palm fibres have a huge potential to be commercialized, specifically by producing highly valued nanomaterial products from agricultural waste. The utilization of this particular waste in bionanocomposite applications is one of the innovative ideas in solving the problem of underutilized renewable materials, hence generating a non-food market product for the agricultural industry [6,23–29]. It is well known from various literature that nanocellulose sourced from other conventional sources displays high stiffness and Young's modulus as high as 150 GPa [1]. Meanwhile, the tensile strength of the NFC is assumed to be approximately from 2 to 4 GPa [1]. Hence, an attempt has been made to isolate nanocellulose from sugar palm fibres and compare its properties with the values obtained so far from other conventional resources. This also offers an opportunity with regards to an effective disposal of the waste. Therefore, the present study aims to isolate NFC from an underutilised and waste raw material that is renewable, recyclable, inexpensive, and abundant in nature. So far, no work has been done regarding the extraction of NFC nanofibres from sugar palm fibres. Therefore, the current study was done and it had successfully isolated nanofibres of NFC from sugar palm fibres through chemo-mechanical treatments, by using HPH and assisted with delignification, mercerization, and refining pre-treatments. The morphological, structural, physico-chemical, and thermal properties of the sugar palm NFC were subsequently analyzed using field emission scanning electron microscopy (FESEM), transmission electron microscopy (TEM), atomic force microscopy (AFM), Brunauer-Emmett-Teller (BET) analysis, degree of polymerization (DP), zeta potential, X-ray diffraction (XRD), Fourier Transform Infrared (FT-IR) spectroscopy, density, moisture content, and thermogravimetric analysis (TGA).

2. Materials and Methods

2.1. Materials

Sugar palm fibres (SPF) were collected from Bahau District, Negeri Sembilan, Malaysia. The chemical reagents utilized included sodium chlorite, ethanoic acid and sodium hydroxide (purchased from Sigma-Aldrich, Malaysia).

2.2. Cellulose Extraction

Sugar palm derived-cellulose was isolated from SPF by using delignification and mercerization processes [30]. The standard method of ASTM D1104-56 was applied to synthesize the holocellulose via delignification [31]. The resulting fibres were known as holocellulose, or sugar palm acid-treated fibres (SPATF). Afterwards, the holocellulose

130 was converted to α-cellulose using ASTM D1103-60 standard [31]. The generated fibres
131 were consequently known as sugar palm cellulose (SPC).

2.3. Isolation of Sugar Palm Nanofibrillated Cellulose (SPNFC)

133 2.3.1. Mechanical pre-treatment

134 A refining treatment prior to the HPH was required in order to enhance fibre accessibility
135 and processing efficiency. Hence, the SPC was refined by 20,000 revolutions in a PFI-
136 mill according to ISO 5264-2:2002 [32]. The process of refining the fibres resulted in the
137 improvement of both external and internal fibrillation. Moreover, this process had
138 improved the flow of fibre and avoided clogging during fluidization. The resultant fibres
139 were known as sugar palm refined fibres (SPRF).

2.3.2. Mechanical high pressurized homogenization (HPH)

141 NFC from sugar palm fibre cellulose was isolated by the process of high pressurized
142 homogenization (HPH). Typically, 1.8 % fibre suspension in water was processed in a
143 high pressurized homogenizer (GEA Niro Soavi, Panda NS1001L, Parma, Italy). The
144 samples were passed 15 times through an intensifier pump that had increased the pump
145 pressure, followed by the interaction chamber. This chamber had subsequently
146 defibrillated the fibres by shear forces and impacts against the channel walls and colliding
147 streams. Through the process, fibres were broken down from macro-sized structures to
148 nano-sized structures, forming slurries of NFC. The high pressurized homogenizer was
149 maintained to operate at 500 bar, whereas the fibrillation was conducted under neutral
150 pH. The temperature was not controlled, but fluidization was temporarily stopped when
151 the temperature of the stock reached approximately 90 °C to prevent pump cavitation.
152 The process was then continued when the samples had cooled to approximately 45°C.
153 Afterwards, ethylene gas at the temperature of -110°C was used to freeze-dry the
154 SPNFCs suspensions. Then, dried SPNFCs were collected and kept in a cool place for
155 sample analysis.

2.4. Methods of Characterization

157 2.4.1. Chemical composition determination

158 Treatment stages like raw fibres, acid-treated fibres, alkali-treated fibres and refined fibre
159 were respectively considered for the determination of SPF's chemical compositions.
160 Wise, Murphy, and D'Addieco method [33] was specifically used to determine the
161 percentage of holocellulose. Meanwhile, the TAPPI standard techniques, namely T 222
162 (acid-insoluble lignin in wood and pulp) [34] and T 203 (alpha-, beta- and gamma-
163 cellulose in pulp) [35] were simultaneously used for the determination of lignin (acid
164 insoluble) and α-cellulose content in fibres.

2.4.2. Field emission scanning electron microscopy (FESEM)

166 The microstructure and nanostructure topography of the longitudinal cross section of
167 SPFs, treated fibres, and SPNFCs were visualized with the aid of the FEI NOVA
168 NanoSEM 230 machine (FEI, Brno-Černovice, Czech Republic), which possessed 3 kV
169 accelerating voltage. A precautionary step to avoid over-charging was performed by

170   coating the samples with gold.

2.4.3. Transmission electron microscopy (TEM)

TEM analysis was used to view the nanostructural images of the SPNFCs using a Philips Tecnai 20 machine with 200 kV acceleration voltage. Initially, dried SPNFCs were dispersed in distilled water and sonicated for 10 min to generate the SPNFCs' suspension. Afterwards, a drop of SPNFCs suspension was mounted on a carbon-coated metallic copper grid and was left to dry at room temperature.

2.4.4 Atomic force microscopy (AFM)

The AFM analysis was performed by using dimension edge with high-performance AFM tool (Bruker, Santa Barbara, CA, USA) in assistance of a software known as Bruker Nanoscope analysis (Version 1.7). It functioned using the Peak/Force tapping mode with a single controller (Nanoscope V from Bruker) for the estimation of the SPNFCs' thickness. A drop of SPNFCs suspension was dropped on the surface of an optical glass slide and was left to air dry. Then, the SPNFCs samples were scanned at room temperature and within controlled relative humidity in the tapping mode of the machine with OMCL-AC160TA standard Si probes (radius of tip less than 10 nm, spring constant of 2.98 N/m and resonant frequency of ~310 kHz) under a scan rate of 1 Hz.

2.4.5. Yield

Solid content (Sc) about 0.2% was diluted with distilled water and centrifuged at 4500 rpm for 20 min before being dried to a constant weight at 90 °C in a halogen desiccator. The yield was then calculated using Eq.(1), where % Sc was solid content percentage. The results represented the average values of three replicates.

$$\text{Yield \%} = \left(1 - \frac{weight\ of\ dried\ sediment}{weight\ of\ diluted\ sample\ \times\ \%Sc} \right) \times 100 \tag{1}$$

2.4.6. Density

Gas intrusion under helium (He) gas flow and aided by an AccuPyc1340 pycnometer (Micromeritics Instrument Corporation, Norcross, GA, USA) was used to identify the samples' densities. The samples of SPFs, treated fibres and SPNFCs, respectively, were oven-dried at a temperature of 105 °C for 24 h to eliminate the moisture within the fibres. Then, these oven-dried fibres were placed into the desiccator to prevent absorption of atmospheric moisture prior to their insertion into the pycnometer. Five replicates of measurements were subsequently performed at a temperature of 27°C and the mean values were then evaluated.

2.4.7. Moisture content

The moisture content experiment was carried out using five (5) prepared samples. All samples were kept in the oven at a temperature of 105 °C for a period of 24 h. The initial weight of the samples prior to the oven-drying process, M_i *(g)* and the final weight after

206 the process, M_f *(g)* were measured so as to evaluate the moisture content. The
207 computation of the moisture content of the samples was done with the aid of Eq.(2).

208 Moisture content (%) = $\dfrac{M_i - M_f}{M_i} \times 100$ (2)

2.4.8. Porosity and surface area measurements

The N_2 adsorption-desorption or Brunauer-Emmet-Teller (BET) technique at 77 K with employment of a porosity and surface area analyzer BELSorp Mini II (NIKKISO, Osaka, Japan) was used to measure the surface area, size of pores, and their respective distribution. With the aid of the vacuum operating condition of 105°C temperature for a period of 10 h, the samples were degassed. BET equation aided relative P/P_o pressure range of 10-20 to 1 was used to attain specific surface areas from the linear portion of the isotherms. In the meantime, Barrett-Joyner-Halenda (BJH) technique was used to determine distribution of pore size from the adsorption branch of the isotherms. The amount adsorbed at a relative pressure of $P/Po = 0.98$ was used to estimate the total pore volume.

2.4.9. Degree of polymerization (DP)

Degree of polymerizations (DP) of the various samples of fibre suspension, such as SPF, SPATF, SPC, SPRF and SPNFCs, were respectively resolved based on their intrinsic viscosity [η]. The TAPPI standard method T230 om-08 [36] and ISO 5351 [37] were employed in the viscosity measurement of the highlighted fibre suspensions' samples. The fibre suspension, copper (II) ethylenediamine (CED) solution and distilled water were mixed together in the ratio 0.01:1:1, respectively, with CED serving as the main dissolution agent. The resultant mixture was cautiously shaken to ensure complete dissolution of the fibre suspension. The viscosity determination was then performed using Ubbelohde viscometer tube (Type 231, PTA Laboratory Equipment, Vorchdorf, Austria) on the produced solution and the initial solvent at 25 °C. Similar determinations were also carried out on the other fibre samples in triplicates. The Mark-Houwink approach, as related in Eq.(3), was used in the computation of the molecular weight of treated fibres, where [η] is the intrinsic viscosity and M is the molecular weight. The constant values of α and K had values of 1 and 0.42 for CED solvent, respectively.

$$[η]=KM^α \tag{3}$$

2.4.10. Fourier Transform Infrared (FTIR) spectroscopy

The detection of possible changes in the existing sugar palm fibres' functional groups at different treatments was carried out with the aid of FT-IR spectroscopic measurements (Nicolet 6700 AEM, Thermo Nicolet Corporation, Madison WI, USA) within the range of 500–4000 cm^{-1}. The samples were mixed with potassium bromide and pressed into thin transparent films that were then subjected to FT-IR analysis.

2.4.11. X-ray diffraction (XRD)

The investigation of the raw fibres, treated fibres and nanofibres x-ray diffraction was determined using Rigaku D/max 2500 X-ray powder diffractometer (Rigaku, Tokyo, Japan), equipped with CuKα radiation (λ=0.1541 nm) in the 2θ range 5–50°. The crystallinity index of each fibre sample Xc, as depicted in Eq.(4), can be deduced from the empirical method reported by Asrofi et al. [38] I_{am} and I_{002} are the peak where

248   intensities of the amorphous and crystalline materials, respectively.

$$X_c = \frac{I_{002} - I_{am}}{I_{002}} \times 100$$

2492
4
9
(4)

2.4.12. Zeta Potential

The determination of the SPNFCs' size along with the characterization of the nanofibre surface charge property were carried out with the aid of Zetasizer Nano-ZS (Malvern Instruments, Worcestershire, United Kingdom). Each fibre sample was diluted by ten-fold in distilled water to 1 ml total volume and then placed into a particle size analyzer at room temperature (25°C). The analysis employed the electrophoretic mobility (μm/s) of the nanofibres, which was converted to zeta potential using an in-built software based on the Helmholtz-Smoluchowski equation.

2.4.13. Thermogravimetric analysis (TGA)

TGA analyzer was used to investigate the thermal stability of the fibres, with respect to weight loss due to increase in temperature. In order to investigate the thermal degradation of sugar palm fibres at varying fibre treatments, the operating conditions were commonly set at a range of temperature of 25–600 °C, with the aid of a dynamic nitrogen atmosphere, and 10 °C heating rate, as well as conducting the analysis by depositing the fibre samples in aluminium pans.

3. Results and Discussion

266266

3.1. Morphological Study of Sugar Palm Fibres and Treated Fibres

268268

Fig. 1. Photographs of (a) the sugar palm tree, (b) raw sugar palm fibers, (c)

bleached fibres, (d) alkali-treated fibres, and (e) refined fibres.

271271

Fig. 2. FE-SEM micrographs of (a) longitudinal section of raw sugar palm fibres, (b)

cross section of raw sugar palm fibres, (c) primary, secondary cell wall and middle
lamella, (d) bleached fibres, (e) alkali-treated fibres, and (f) refined fibres.

275275

Fig. 1 displays the sugar palm tree and its fibres at different stages of treatment. The sugar palm fibres colour changed from black (Fig. 1b) to brown after the bleaching

278   treatment (Fig. 1c) and became white after alkali and refined treatments, respectively (Fig.
279   1e). FESEM micrographs of the cross and longitudinal section of the sugar palm fibres
280   are represented in Fig. 2a, b, and g. The FESEM micrographs also displayed partial
281   elimination of amorphous regions like hemicellulose, lignin, and pectin after the chemical
282   treatment. These substances had acted as reinforcing components covering the fibre
283   bundles.

284   The SPF longitudinal section surface morphology was found to be uneven, with pore-like
285   spots that appeared in most regular intervals (Fig. 2 a). These spots could also be found

on coir fibre surfaces [39]. The clarity of the exterior surface of the fibres was a result of the removal of the waxy layer present on their exterior surface [40–42]. The mean diameter of the bleached fibres was reduced after the chemical treatment, from 212.01 ± 2.17 μm to 121.80 ± 10.57 μm, which was attributable to the partial removal of lignin and hemicellulose. After the alkali treatment (Fig. 2 e), the fibre bundles were dispersed into individual micro-fibres with the diameter of 11.87 ± 1.04 μm. In comparison, the diameter of raw sugar palm fibres doubled than that of bleached fibres, and was eighteen times larger than the alkali-treated fibres. In addition, the surface morphology of the raw SPC changed to smooth and groovy surfaces, along with parallel arrangement along the cellulose (Fig. 2 d). Similar results were also reported by other authors, such as the average diameter of sisal cellulose (13.5 μm) [43] and kenaf-derived cellulose (13 μm) [44]. Similarly, microfibrillation of the sugar palm fibres after refining using PFI-mil is shown in (Fig. 2 f). During the mechanical refining process, the microfibrils were pulled out from the fibres' cell wall due to the shearing action on their surfaces [45]. The sugar palm cellulose pulp was then beaten by the pressure present between the wall and the bar, in which a constant load was given to the pulp circulating between a stainless steel roll and cylindrical mill house. Their rotation with a constant difference in circumferential velocity had applied mechanical effects, such as shear and compression, thereby performing refining actions via frictional forces between the fibres. The microfibrils in this image displayed an average of 3.93 ± 0.26 μm in diameter, which was 55 times thinner than the raw sugar palm fibres. The refining process was commonly applied as a mechanical pre-treatment during the first stage of NFC production. It increased the fibre's specific surface and volume, as well as making the microfibrils more accessible for further mechanical treatment of HPH.

310

3.2. Chemical analysis of Sugar Palm Fibres and Treated Fibres

312

Table 1 Chemical constituent of sugar palm fibres at various stage of treatment.

314

Table 1 displays the chemical composition of sugar across different stages of treatment. After treating the fibres with $NaClO_2$ solution, the lignin content was reduced by 32.97%, whereas the cellulose was only reduced by about 12.79%. The alkali treatment affected the content of hemicellulose, which was reduced to 3.97%, while the cellulose increased by 25.66% that is almost two-fold compared to the acid-treatment fibres. This was caused by the cleavage of the ester-linked substances of hemicellulose [46]. In addition, the chemical treatment also allowed an increment in the surface area of the SPFs, thus making the polysaccharides defibrillating easily under high shear force. Meanwhile, the mechanical refining treatment, PFI-mill contributed to the defibrillation of SPFs by cleaving the inter-fibrillar hydrogen bonds between the nanofibril and caused the cellulose content to increase from 82.33% to 88.79%. This result was similar to the one reported earlier by Hai, Park and Seo [47], who indicated that the PFI-mill refining process affected

13

327   the cellulose content. The contents of cellulose, hemicellulose, and lignin after refined
328   treatment were 88.79%, 0.04%, and 3.85%, respectively.

3.3. Isolation of SPNFCs

331331

Fig. 3. (a) 2 wt% of nanocellulose suspension (b) field emission scanning electron

microscopy (FESEM) micrograph, (c) height dimension of NFCs by means of
atomic force microscopy (AFM) nanograph, (d) transmission electron microscopy

(TEM) nanograph, (e) atomic force microscopy (AFM) nanograph, and (f and g)
their diameter histograms based on TEM and AFM nanograph.

The nanocellulose suspension prepared from purified sugar palm fibres is shown in Fig. 3 (a). The concentration of this suspension was 2 wt%. The FESEM observation and height of nanocellulose are shown in Fig. 3 (b) and Fig.3 (c), respectively. TEM and AFM observations and their distribution of diameters are shown in Fig. 3 (d and f) and Fig. 3 (e and f), respectively. The defibrillation of sugar palm cellulose fibres to obtain nanoscale web-like termed as NFC was obtained by using a chemical pre-treatment and subsequent mechanical treatment of cellulose fibres. This consisted of pulp beating/refining (PFI-mill) and HPH processes. The yield of nanofibrils collected during the process of defibrillation was very high, with 92% nanofibrous elements having diameters values of 5.5 ± 1.0 nm (TEM) and 9 ± 2 nm (AFM) (Fig. 3 f and g). The micrographs also resembled "noodle-like nanofibres" (Fig. 3e). The larger fibre diameter displayed in Fig. 3 (e) may have resulted from a tip coardening effect, which was often associated with AFM. The height of the SPNFCs was recorded at 10.17 nm, whereby the value was close to the average nanofibre diameter (9 ± 2 nm) calculated from the AFM images. This obtained the yield of SPNFCs was in good agreement with the yield of eucalyptus wood (96%) and pine wood (88%) as reported by Besbes et al. [48]. Similar results of the diameters were reported by other authors on agro residue sources like banana (5 nm) [49] and flax fibres (5 nm) [50]. By comparing the microscopy images among TEM, FESEM and AFM, it could be deduced that TEM resulted in the clearest insight regarding the resultant NFCs morphology with widths that were the size of 5.5 ± 1.0 nm. Additionally, it is well known that AFM is usually carried out for accurate measurement of the thickness of the nanofibres. Furthermore, the aqueous suspensions of NFCs were determined to be stable (Fig. 3 d) due to the presence of evenly distributed negative charges, thus preventing agglomeration [51]. The negative charges induced electrostatic repulsion forces among the nanoparticles. This repulsive force kept the nanoparticles from collapsing into one another, thereby maintaining the stable suspension [52]. Meanwhile, the zeta potential analysis estimated the value of the negative charge on the SPNFCs to be -34.2 mV. These large negatively-charged zeta potential values were obtained due to the properties of the cellulose fibres, which contained –OH functional groups and gave the polymer its negative charge. The suspension of NFCs was considered stable as its absolute value was lesser than -30 mV and greater than 30 mV [53]. Therefore, all of these were considered as imperative qualities in the incorporation of NFCs as nano-reinforcement agents within the nanocomposites of a polymer.

370370

371 ## 3.4. Physical Properties

372 **Table 2 Physical properties of SPF** [54], **SPATF** [54], **SPC** [54], **SPRF, SPNFCs, and**
373 **others nanofibres.**

374 Table 2 shows the physical properties (i.e. diameter, density, moisture content, degree of
375 crystallinity, surface area, degree of polymerization and molecular weight) of untreated
376 and treated fibres. It can be seen from Table 2 that the moisture content percentage had
377 increased from raw sugar palm fibre (8.36 ± 0.10 %) to SPNFCs (12.86 ± 0.89 %). This
378 may be attributed to the surface structure of cellulose that comprised of abundant
379 hydroxyl groups known to be very sensitive to water molecules. The fibre surfaces were
380 revealed to have abundant formations of hydrophilic ionic groups due to the treatments
381 that were carried out during the process of bleaching, alkalinisation, refining, and HPH.
382 Besides, voids were created within the fibre structure, thereby led to fibres swell and to
383 become well-separated. Therefore, the value of density decreased as the volume
384 increased along with the loss in weight. In comparison with manmade fibres like glass
385 fibre, aramid and carbon having density values of 2.5 g/cm^{-3}, 1.4 g/cm^{-3} and 1.7 g/cm^{-3},
386 respectively, SPNFC possessed a lower density value. Besides, the density of the fibre
387 was also interrelated to its porosity and surface area; when the pore volume of the fibre
388 increased, the fibre density would decrease. From the analysis, it could be concluded that
389 all fibres displayed type IV isotherms accompanied by hysteresis loop, which were linked
390 with capillary condensation that was taking place in mesopores (2–50 nm). Furthermore,
391 the fibres also showed an increasing trend in cumulative pore volumes of sugar palm fibre
392 (SPF) (0.061 cm^3/g) to SPNFC (0.211 cm^3/g). The increasing trend of cumulative pore
393 volume was due to the fact that the SPF possessed closely aligned, rigid, and strong-
394 bound building elements through hydrogen bonded cellulose structure, which was a result
395 of the parting small interfacial spaces [55]. Through the mechanical treatment, opening
396 of fibre-bundles and defibrillation of individualized SPF that occurred was indirectly
397 decreasing the size of the fibre from micro to nano-scale. This also resulted in an increase
398 of the interfacial spaces between the nanofibrils. The BET surface area of the fibres also
399 showed similar increasing trends as the cumulative pore volume. It was estimated that
400 the surface area of SPNFCs was four times greater than SPF, which was higher and
401 attributed to the nanosize SPNFCs as compared to macro-sized SPF.

402 Besides, Table 2 indicates that the DP and molecular weight of the fibres were reduced
403 significantly from bleached fibre to SPNFCs, from 2,963.33 to 289.79, and from
404 480,513.39 g/mol to 46,989 g/mol, respectively. The decreasing trend observed for the
405 degree of fibre polymerization was attributed to the removal of lignin, hemicellulose, and
406 inter-fibrillatedhydrogen bonds between nanofibrils. This occurred due to the
407 delignification, mercerization, refining, and HPH of the SPF. DP obtained for the SPNFCs
408 was almost similar to the DP of beech wood (*Fagus sylvatica*) nanofibril (230) [56], higher
409 than sugar beet pulp (120) [57], and lower than oil palm mesocarp microfibril (967) [58],
410 soft wood of spruce (*Picea abies*) nanofibril (825), softwood (480) [59], wheat straw
411 (*Triticum sp.*) nanofibril (674) [56], and empty palm fruit bunch (EPFB) (489 ± 23) [60].

412412

413 # 3.5. FTIR spectroscopy analysis

Fig. 4. Fourier-transform infrared spectroscopy of (a) raw sugar palm fibre [54]**, (b) bleached fibre** [54]**, (c) alkali-treated fibre** [54]**, (d) refined fibre, and (e) sugar palm nanofibrillated cellulose.**

Fig. 4 displays the FTIR spectra of SPF, acid-treated fibres, alkali-treated fibres, refined fibres, and nanofibrillated cellulose (NFCs). The intense peaks at $3100–3700$ cm^{-1} were assigned to the adsorbed water, which also depicted the presence of hydroxyl groups in all fibres. Besides, there were many hydrogen bonded networks or hydroxyl functional groups on the surface of NFCs, corresponding to the hydroxyl stretching vibration at the $3100–3700$ cm^{-1} region. These intense peaks remained in the NFCs peak after several treatments going on the raw SPF, whereas the intensity of the O-H groups peaked as the fibres were treated from raw fibres, bleached fibres, alkali treated fibres, refined fibres to NFCs. These occurrences were due to the large surface area exposed by the fibres, and resulting from the size reduction of the fibre dimension. Moreover, the presence of cellulose could be determined via the intense peak located at 897 cm^{-1} (C–H rocking vibrations), 1030 cm^{-1} (C–O stretching), 1160 cm^{-1} (C–O–C asymmetric valence vibration), 1316 cm^{-1} (C–H$_2$ rocking vibration), 1370 cm^{-1} (C–H$_2$ deformation vibration), and 1424 cm^{-1} [54].

The absorbance bands located at 1593 cm^{-1} , 1507 cm^{-1} and 1227 cm^{-1} were observed in the raw SPF, which indicated the CηC stretching of the aromatic rings of lignin [61]. However, these peaks were noted to disappear when the fibres underwent acid treatment of delignification process, signifying that such chemical process successfully eliminated lignin from the fibre composition. In addition, the absorbance peak of $1000–1300$ cm^{-1} was observed to appear in all untreated and treated fibres, indicating the presence of C-O and C-H stretching groups [62].

3.6. X-ray diffraction measurements

Fig. 5. XRD arrays of (a) raw sugar palm fibres [54]**, (b) bleached fibres** [54]**, (c) alkali-treated fibres** [54]**, (d) refined fibres, and (e) SPNFCs.**

441441

Fig. 5 shows XRD patterns for sugar palm fibres at different stages of treatment. A well-defined mixture of cellulose I polymorph ($2\theta=15°$ and $22.6°$) was observed in SPNFCs XRD pattern, with amorphous regions characterized at the small intensity peak at a $2\theta=18°$. There was no presence of polymorphs of cellulose II ($2\theta=12.3^{'}$ and $22.1^{'}$) in the X-ray diffraction. Cellulose I was the most stable structure compared to cellulose types II, III and IV [53]. The crystallinity index of fibres was observed to increase from 55.8 % to 81.2 %. The increment of the fibre crystallinity index was due to the removal of non-cellulosic compounds of fibre (lignin and hemicellulose) by chemical and mechanical treatments. Furthermore, the humps were reduced after alkali-treatment showing that the amorphous chains had been arranged into crystalline regions. The larger crystallinity index can be known by observing the sharpness of the peak [63]. Similarly, it could also be comprehended from the diffractogram of cellulose, in which the sharpness in the edge of the diffractogram for the nanofibres had greatly increased. Moreover, the crystallinity index of SPNFCs was observed to be similar to kenaf bast fibre (*Hibiscus cannabinus*

456   *v36*) (81.5%) [64], and higher than pine (75%) [48]. Thus, it could be concluded that the

crystallinity values were different due to the plant's origins, as well as the types and
variables of fibre purification used to disintegrate the fibres.

3.7. Thermogravimetric analysis (TGA)

460460

Fig. 6. (i) Thermogravimetry (TG) and (ii) derivative thermogravimetric (DTG) curves

for (a) raw sugar palm fibres [54], **(b) bleached fibres** [54], **(c) alkali-treated fibres** [54], **(d) refined fibre and (e) SPNFCs.**

Table 3 Decomposition temperature of SPF[54], **SPATF**[54], **SPC**[54], **SPRF, and SPNFCs.**

Table 3 shows the thermogravimetry (TG) and derivative thermogravimetric (DTG) curve of untreated and treated fibres. Since the thermoplastic processing temperature will rise beyond 200°C, therefore studying the thermal properties (i.e. TFA and DTG) of the natural fibres were crucial to determine their compatibility as nanofillers for bio-composite processing. Fig. 6 displays the TGA (i.e. TG-panel (i) and DTG- panel (ii)) outcomes for SPF, SPATF, SPC, SPRF and SPNFC fibres, respectively. The percentage of weight loss for all sugar palm fibres was compared and displayed accordingly in Table 3. It was noted that the decomposition temperature of SPF had basically taken place in four (4) stages [54]. The first stage was referred to as the evaporation stage, which occurred in the temperature range of 45–123°C and in which the moisture contained in the fibres was evaporated. The second stage was the decomposition stage occurring at around 220 °C to approximately 315 °C, in which the lignocellulosic components of hemicelluloses contained in the fibres were decomposed. Closely following this stage was the 3rd stage of cellulose decomposition, which was in the temperature range of 315 °C to ~ 400 °C, and followed by the fourth stage. The final stage witnessed the elimination of lignin in the temperature range of 165 °C to ~ 900 °C, and lastly, ash formation at 1723 °C.

The evaporation of moisture content in fibres within the temperature range of 29–42 °C marked the beginning of fibre weight loss and the weight reduction continued as the fibres were heated. The movement of water and volatile extractives that occurred may be a result of the water molecule migration, which also carried extractives from the internal part of the fibres to their external part (i.e. fibre surfaces) [65]. Furthermore, the evaporation of water molecules from the raw SPF and treated fibres took place at 196.56 °C and 134–189 °C, respectively (Fig. 6). The difference of the temperature may be perceived as an indicator of the varying moisture content within raw and treated SPF, accordingly. The highest moisture content (MC) was attained by raw fibre (10.38%) in comparison to the treated fibre. Upon treating the fibres, the MC decreased and led to correspondingly low weight loss. Such low weight losses may be adduced to the minimal loss of volatile extractives in the fibres, which was also linked to low heating temperature. The MC of the cell lumen and cell wall were equally small, but severe weight loss of approximately up to 70% might be attributable to the main components of the fibres (i.e. hemicellulose, cellulose and lignin). This was due to their role being the location where the decomposition process took place at temperature of 100 °C and above [65]. Besides, the weight loss of SPNFCs was higher than SPRF due to the surface structure of

499   cellulose, which comprised of abundant hydroxyl groups known to be very sensitive to

water molecules. The degradation of hemicellulose constituted as the second stage of the entire process. Usually, hemicellulose was readily converted into CO_2, CO, and some hydrocarbons at the low-temperature ranges of 220 °C to 315 °C. Therefore, the DTG curve of SPF fibre presented an initial weight loss that commenced at 210.58 °C before continuing to the highest temperature of 281 °C. These values were suggestive of low degradation temperature of lignin and hemicellulose [66]. Similarly, the delignification process encouraged the expulsion of fibre components, such as lignin, hemicelluloses, and waxes, thereby giving rise to high surface having well-defined fibril aggregates. Meanwhile, the low percent composition of lignin in the SPATF fibres compared to that of raw SPF as revealed in Table 3 was suggestive of a reduction in the value of the temperature of acid-treated fibres. Additionally, lignin is a very difficult component to degrade (160–900 °C) in the raw SPFs, which functioned as the agent of stiffness to the cell wall and cemented individual cells together in the middle lamella region of the fibres [65]. Following the elimination of the lignin from the raw SPFs via the bleaching process, the leftover chemical substances in the fibres were mainly composed of hemicellulose and cellulose. Therefore, the low degradation temperature of hemicellulose (220–315 °C) in comparison to other macromolecules like cellulose and lignin suggested for its readily decomposing function within the alkaline medium. The small peaks that appeared at 281 and 271.56 °C in the neighbourhood of the main peak during the degradation of (a) SPF, and (b) SPATF, respectively, may be ascribed to the presence of hemicellulose and lignin. However, these peaks were not visible in the SPATF and SPNFCs. The weight losses were also observed to be much more progressive in the raw SPFs than that of the treated fibres. Besides, the observed shoulder in DTG analysis at around 300 °C for the raw SPFs was missing in the alkali-treated fibres, indicating the partial removal of the hemicellulose [46].

The degradation of cellulose took place at the third stage, which commenced at the temperature range of 315–400 °C [67]. Furthermore, alkali-treated fibres (c) unveiled a rise in the weight loss during the first degradation (W_L=73.71%; T_{Max}=346.09) and second degradation (W_L=43.76%;T_{Max}=345.45), in comparison with the raw SPFs and the second degradation of SPATF (W_L=52.39%;T_{Max}=324.44). The alkali-treated fibres produced cellulose fibres with a high decomposition temperature at around 346 °C. Such outcome may be attributed to the partial elimination of hemicellulose and lignin during the bleaching process, as shown in Table 1. This result also verified cellulose's capability to withstand high-temperature deformation process. Meanwhile, the alkali-treatment stage involved the oxidation of lignin and hemicellulose to yield simple sugars, which subsequently released the cellulose fibres [40,41,68]. The decomposition temperature of treated fibres was around 200 °C, which was smaller than raw SPFs. Similar results were also reported on mulberry bark celluloses by Li et al. [69] and pure celluloses by Soares, Camino, and Levchik [70]. The decomposition temperature decreased due to the removal of the lignin and the strongly binding macromolecule of the fibres, thus leaving behind the hemicellulose constituent after the chemical treatment of the fibres. Hemicellulose was often present between and within cellulose fibrils. Therefore, the relatively strong reinforcement between hemicellulose and cellulose fibril gave rise to the reduced cellulose fibril crystallinity, thus speeding the thermal degradation process. The thermal data in Table 3 reveals that SPRF had a low thermal decomposition (T_{max}) of 345.77 °C compared to the SPNFCs sample, attributable to the difference in crystalline organisation.

Meanwhile, SPNFCs displayed gradual thermal transitions in the temperature region of 190–380 °C, whereby it was fundamentally related to the cellulosic chain degradation. Similarly, the T_{max} of SPNFCs (347.40 °C) was greater than that of NFC extracted from commercialised MCC, as reported by Li et al. [71] and had obtained DTG peak temperature T_{max} of 238 °C. Thus, the obtained SPNFCs reaffirmed good thermal stability that was comparable to that of NFC obtained from eucalyptus pulp (307.9 °C), as per the investigations conducted by Wang et al. [72], respectively. Besides, these results may also be due to the highly crystalline organization of the treated fibres, which strengthened the fibres in withstanding severe processing conditions like high temperature. Besides, HPH process was successful in reducing the micro-size fibre chain into nano-size fibres with the application of high shear force on the fibres. Hence, the outcomes from this study confirmed that the SPNFCs displayed thermal property improvements for treated fibres in comparison with the untreated fibres. They consequently supported the nanofibre's suitability as reinforcing materials in the preparation of renewable bio-composites. Polymer biocomposites with high thermal property can be potentially utilised in various applications. The decomposition of lignin within the fibres predominated the fourth stage, which was quite difficult, unlike the degradation of hemicellulose and cellulose. This was due to the wide range of temperature (160 °C to 900 °C) involved in the process, as lignin possessed rigid structure that supported plant fibres and bonded individual cells together in the middle lamella portion of the fibres. However, the decomposition of lignin took place at a rather low weight loss rate (< 0.14 wt.%/°C) from the ambient temperature to 900 °C [65]. Additionally, Fig. 6 also unveils the slight differences in the TG and DTG curves of the treated and untreated fibres. The second SPF curve shifted to the right upon comparison with the SPATF curve. Such observation may be due to the high content of lignin (33.24%) found in the SPF fibres compared with the SPATF (0.27% to 2.78%), which prevented the hemicellulose from being easily disintegrated.

The final degradation stage witnessed the process of oxidation and breaking down of the charred residues. These residues with DTG peak above 425 °C were converted to lower molecular weight gaseous products [66]. Following full disintegration of lignin, the remaining residue left was an inorganic material typically referred to as ash content or char residue. The inorganic substance that made up the char residue included silica (i.e. silicon dioxide, SiO_2), which was only decomposable at the elevated temperature of 1723 °C and above [65]. Nonetheless, the SPATF and SPC produced low weight residue compared to that of raw SPF due to the removal of hemicellulose and lignin constituents from both treated fibres. Similarly, the high residual weight of SPNFCs was likely due to the char formation from flame retardant compounds.

4. Conclusions

In this study, NFCs were successfully isolated from sugar palm fibre (*Arenga pinnata (Wurmb) Merr.*) using chemo-mechanical treatment. The average diameter and length of the NFCs were found to be 5.5 nm and several micrometers, respectively. Based on the chemical compositions of the SPF, SPATF, SPC, and SPRF samples, there were significant reduction in the lignin and hemicellulose contents after delignification, mercerization and refining treatments. The presence of cellulose could otherwise be determined through the intense peak located at 897 cm⁻¹ (C–H rocking vibrations), 1030 cm⁻¹ (C–O stretching), 1160 cm⁻¹ (C–O–C asymmetric valence vibration), 1316 cm⁻¹ (C–

591 H2 rocking vibration), 1370 cm^{-1} (C–H2 deformation vibration), and 1424 cm^{-1}.
592 Meanwhile, well-defined cellulose I polymorph peaks at 2θ=15° and 22.6° in the XRD
593 patterns of NFCS indicated an increase of cellulose crystallinity degree. The crystallinity
594 index of fibres was also observed to increase from 55.8 % (SPF) to 81.2 % (SPNFCs).
595 Therefore, it could be concluded that chemical treatments (i.e. delignification and
596 mercerization) followed with HPH were effective to isolate SPNFCs from sugar palm
597 fibres with a high yield of 92%. In this work, a value had been added to the agro-waste
598 material, apart from the generation of eco-friendly SPNFC nanofillers for diversified
599 applications.

600 Acknowledgments

607 **References**

608
609 [1]   Ilyas RA, Sapuan SM, Sanyang ML, Ishak MR, Zainudin ES. Nanocrystalline 610
          cellulose as reinforcement for polymeric matrix nanocomposites and its
potential611 applications: A Review. Current Analytical Chemistry 2018;14:203–25.

612   doi:10.2174/1573411013666171003155624.

613 [2]   Sapuan SM, Ilyas RA, Ishak MR, Leman Z, Huzaifah MRM, Ammar IM, et al.
614   Development of sugar palm–based products: A community project. Sugar Palm
615   Biofibers, Biopolymers, and Biocomposites. 1st ed., First Edition. Boca Raton, FL
:616   CRC Press/Taylor & Francis Group, 2018.: CRC Press; 2018, p. 245–66.

617   doi:10.1201/9780429443923-12.

618 [3]   Ilyas RA, Sapuan SM, Ishak MR, Zainudin ES, Atikah MSN. Nanocellulose
619   reinforced starch polymer composites : A review of preparation, properties
and 620   application. Proceeding: 5th International Conference on Applied Sciences and
621   Engineering (ICASEA, 2018), Capthorne Hotel, Cameron Highlands, Malaysia:
622   Global Academic Excellence (M) Sdn Bhd; 2018, p. 325–41.
623 [4]   Abitbol T, Rivkin A, Cao Y, Nevo Y, Abraham E, Ben-Shalom T, et
al.624   Nanocellulose, a tiny fiber with huge applications. Current Opinion
in 625   Biotechnology 2016;39:76–88. doi:10.1016/j.copbio.2016.01.002.
626 [5]   Abral H, Basri A, Muhammad F, Fernando Y, Hafizulhaq F, Mahardika M, Sugiarti
627   E, Sapuan MS, Ilyas RA, Stephane I. A simple method for improving the
628   properties of the sago starch films prepared by using ultrasonication treatment.
629   Food Hydrocolloids 2019. doi:10.1016/j.foodhyd.2019.02.012.
630 [6]   Asrofi M, Abral H, Kasim A, Pratoto A, Mahardika M, Hafizulhaq F.
631   Characterization of the sonicated yam bean starch bionanocomposites reinforced
632   by nanocellulose water hyacinth fiber (WHF): the Effect of Various Fiber Loading.
633   Journal of Engineering Science and Technology 2018;13:2700–15.

634 [7] Asrofi M, Abral H, Putra YK, Sapuan SM, Kim HJ. Effect of duration of sonication

635   during gelatinization on properties of tapioca starch water hyacinth fiber

636   biocomposite. International Journal of Biological Macromolecules 2018;108:167–

637   76. doi:10.1016/j.ijbiomac.2017.11.165.

638   [8]   Khalil HPSA, Davoudpour Y, Islam MN, Mustapha A, Sudesh K, Dungani R, et al.

639   Production and modification of nanofibrillated cellulose using various
mechanical 640   processes: A review. Carbohydrate Polymers 2014;99:649–65.

641   doi:10.1016/j.carbpol.2013.08.069.

642   [9]   Syafri E, Kasim A, Abral H, Sudirman, Sulungbudi GT, Sanjay MR, et al.

643   Synthesis and characterization of cellulose nanofibers (CNF) ramie reinforced

644   cassava starch hybrid composites. International Journal of Biological

645   Macromolecules 2018;120:578–86.
doi:10.1016/j.ijbiomac.2018.08.134. 646   [10]   Syafri E, Kasim A, Abral H,
Asben A. Cellulose nanofibers isolation and

647   characterization from ramie using a chemical-ultrasonic treatment. Journal of

648   Natural Fibers 2018;00:1–11. doi:10.1080/15440478.2018.1455073.

649   [11]   Abdul Khalil HPS, Bhat AH, Yusra AFI. Green composites from sustainable

650   cellulose nanofibrils: A review. Carbohydrate Polymers 2012;87:963–79.

651   doi:10.1016/j.carbpol.2011.08.078.

652   [12]   Dufresne A. Cellulose microfibrils from potato tuber cells : Processing and

653   Characterization of Starch – Cellulose Microfibril Composites. Polymer

654   2000;76:2080–92. doi:10.1002/(SICI)1097-4628(20000628)76:14<2080::AID-

655   APP12>3.0.CO;2-U.

656   [13]   Teixeira E de M, Pasquini D, Curvelo AASS, Corradini E, Belgacem MN, 657   Dufresne A. Cassava bagasse cellulose nanofibrils reinforced
thermoplastic 658   cassava starch. Carbohydrate Polymers 2009;78:422–31.

659   doi:10.1016/j.carbpol.2009.04.034.

660   [14]   Pelissari FM, Andrade-Mahecha MM, Sobral PJ do A, Menegalli FC.

661   Nanocomposites based on banana starch reinforced with cellulose nanofibers

662   isolated from banana peels. Journal of Colloid and Interface Science

663   2017;505:154–67. doi:10.1016/j.jcis.2017.05.106.

664   [15]   Kaushik A, Singh M, Verma G. Green nanocomposites based on thermoplastic

665   starch and steam exploded cellulose nanofibrils from wheat straw.
Carbohydrate 666   Polymers 2010;82:337–45. doi:10.1016/j.carbpol.2010.04.063.

667   [16]   Nasri-Nasrabadi B, Behzad T, Bagheri R. Preparation and characterization
of 668   cellulose nanofiber reinforced thermoplastic starch composites. Fibers and

669   Polymers 2014;15:347–54. doi:10.1007/s12221-014-0347-0.

670   [17]   Abraham E, Deepa B, Pothen LA, Cintil J, Thomas S, John MJ, et al.

671   Environmental friendly method for the extraction of coir fibre and isolation of

672   nanofibre. Carbohydrate Polymers 2013;92:1477–83.

673   doi:10.1016/j.carbpol.2012.10.056.

674   [18]   Li M, Wang LJ, Li D, Cheng YL, Adhikari B. Preparation and characterization of

675   cellulose nanofibers from de-pectinated sugar beet pulp. Carbohydrate

Polymers676 2014;102:136–43. doi:10.1016/j.carbpol.2013.11.021.

677   [19]   Valdebenito F, Pereira M, Ciudad G, Azocar L, Briones R, Chinga-Carrasco G.

678   On the nanofibrillation of corn husks and oat hulls fibres. Industrial Crops

and 679   Products 2017;95:528–34. doi:10.1016/j.indcrop.2016.11.006.

680   [20]   Sapuan SM, Ishak MR, Leman Z, Ilyas RA, Huzaifah MRM. Development of

681   products from sugar palm trees (*Arenga Pinnata Wurb. Merr*): A community

682   project. INTROPica 2017:12–3.

683   [21] Radzi AM, Sapuan SM, Jawaid M, Mansor MR. Influence of fibre contents on
684   mechanical and thermal properties of roselle fibre reinforced polyurethane
685   composites. Fibers and Polymers 2017;18:1353–8. doi:10.1007/s12221-017-
686   7311-8.

687   [22] Jumaidin R, Sapuan SM, Jawaid M, Ishak MR, Sahari J. Effect of seaweed on
688   physical properties of thermoplastic sugar palm starch/agar composites.
Journal689 of Mechanical Engineering and Sciences 2016;10:2214–25.

690   doi:10.15282/jmes.10.3.2016.1.0207.

691   [23] Sanyang ML, Ilyas RA, Sapuan SM, Jumaidin R. Sugar palm starch-based
692   composites for packaging applications. Bionanocomposites for Packaging
693   Applications, Cham: Springer International Publishing; 2018, p. 125–47.

694   doi:10.1007/978-3-319-67319-6_7.

695   [24] Ilyas RA, Sapuan SM, Ishak MR, Zainudin ES. Development and characterization

696   of sugar palm nanocrystalline cellulose reinforced sugar palm starch

697   bionanocomposites. Carbohydrate Polymers 2018;202:186–202.

698   doi:10.1016/j.carbpol.2018.09.002.

699   [25] Ilyas RA, Sapuan SM, Ishak MR, Zainudin ES. Sugar palm nanocrystalline

700   cellulose reinforced sugar palm starch composite: Degradation and water-barrier

701   properties. IOP Conference Series: Materials Science and Engineering

702   2018;368:012006. doi:10.1088/1757-899X/368/1/012006.

703   [26] Ilyas RA, Sapuan SM, Sanyang ML, Ishak MR. Nanocrystalline cellulose
704   reinforced starch-based nanocomposite: A review. 5th Postgraduate Seminar on
705   Natural Fiber Composites, Serdang, Selangor: Universiti Putra Malaysia; 2016,
p.706   82–7.

707   [27] Ilyas RA, Sapuan SM, Ishak MR, Zainudin ES, Atikah MSN. Characterization of 708
        sugar palm nanocellulose and its potential for reinforcement with a starch-
based 709 composite. sugar palm biofibers, biopolymers, and biocomposites. 1st ed.,
First 710 Edition. Boca Raton, FL : CRC Press/Taylor & Francis Group, 2018.: CRC Press;
711   2018, p. 189–220. doi:10.1201/9780429443923-10.

712   [28] Ilyas RA, Sapuan SM, Ishak MR, Zainudin ES. Water transport properties of bio-
713   nanocomposites reinforced by sugar palm (*Arenga Pinnata*)
nanofibrillated714 cellulose. Journal of Advanced Research in Fluid Mechanics and
Thermal 715 Sciences Journal 2018;51:234–46.

716   [29] Ilyas RA, Sapuan SM, Ishak MR, Zainudin ES, Atikah MSN, Huzaifah MRM.

717   Water barrier properties of biodegradable films reinforced with nanocellulose
for 718   food packaging application : A review. 6th Postgraduate Seminar on Natural
Fiber719   Reinforced Polymer Composites 2018, Serdang, Selangor: 2018, p. 55–9.

720   [30]   Ilyas RA, Sapuan SM, Ishak MR, Zainudin ES. Effect of delignification on the

721   physical, thermal, chemical, and structural properties of sugar palm fibre.

722   BioResources 2017;12:8734–54. doi:10.15376/biores.12.4.8734-8754.

723   [31]   Sanyang ML, Sapuan SM, Jawaid M, Ishak MR, Sahari J. Effect of sugar palm- 724   derived cellulose reinforcement on the mechanical and water barrier properties of 725   sugar palm starch biocomposite films. BioResources 2016;11:4134–45.

726   doi:10.15376/biores.11.2.4134-4145.

727 [32] ISO 5264-2. Pulps — Laboratory beating — Part 2: PFI mill method 2002.

728 [33] Wise LE, Murphy M, D'Addieco AA. Chlorite, holocellulose, its fractionation and
729 bearing on summative wood analysis and on studies on the hemicellulose.
Paper730 Trade Journal 1946;122:35–43.

731 [34] T 222 om-02. Acid-insoluble lignin in wood and pulp. Tappi 2006.

732 [35] T 203 cm-99. Alpha-, beta- and gamma-cellulose in pulp. Tappi 2009.

733 [36] T230 om-08. Viscosity of pulp (capillary viscometer method). Tappi 2013.

734 [37] ISO 5351:2004(E). Pulps — Determination of limiting viscosity number in cupri-
735 ethylenediamine (CED) solution. International Standard 2004.

736 [38] Asrofi M, Abral H, Kasim A, Pratoto A, Mahardika M, Hafizulhaq F. Mechanical
737 properties of a water hyacinth nanofiber cellulose reinforced thermoplastic starch
738 bionanocomposite: Effect of ultrasonic vibration during processing. Fibers

739 2018;6:40. doi:10.3390/fib6020040.

740 [39] Ticoalu A, Aravinthan T, Cardona F. A review on the characteristics of gomuti

741 fibre and its composites with thermoset resins. Journal of Reinforced Plastics and

742 Composites 2013;32:124–36. doi:10.1177/0731684412463109.

743 [40] Thakur MK, Gupta RK, Thakur VK. Surface modification of cellulose using silane

744 coupling agent. Carbohydrate Polymers 2014;111:849–55.

745 doi:10.1016/j.carbpol.2014.05.041.

746 [41] Thakur VK, Singha AS, Thakur MK. Synthesis of natural cellulose-based graft
747 copolymers using methyl methacrylate as an efficient Monomer. Advances
in 748 Polymer Technology 2013;32:E741–8. doi:10.1002/adv.21317.

749 [42] Thakur VK, Singha AS, Thakur MK. Biopolymers based green composites:

750 mechanical, thermal and physico-chemical characterization. Journal of Polymers

751 and the Environment 2012;20:412–21. doi:10.1007/s10924-011-0389-y.

752 [43] Savastano H, Warden P., Coutts RS. Brazilian waste fibres as reinforcement for
753 cement-based composites. Cement and Concrete Composites 2000;22:379–84.
754 doi:10.1016/S0958-9465(00)00034-2.

755 [44] Tawakkal ISM, Talib R, Abdan K, Ling CN. Mechanical and physical properties of

756 Kenaf-Derived Cellulose (KDC)-filled polylactic acid (PLA) composites.

757 BioResources 2012;7:1643–55. doi:10.15376/biores.7.2.1643-1655.

758 [45] Tonoli GHD, Joaquim AP, Arsène M-A, Bilba K, Savastano H. Performance and
759 durability of cement based composites reinforced with refined sisal pulp.
Materials760 and Manufacturing Processes 2007;22:149–56.

761 doi:10.1080/10426910601062065.

762 [46] Sheltami RM, Abdullah I, Ahmad I, Dufresne A, Kargarzadeh H. Extraction of
763 cellulose nanocrystals from mengkuang leaves (*Pandanus tectorius*).
764 Carbohydrate Polymers 2012;88:772–9. doi:10.1016/j.carbpol.2012.01.062.

765 [47] Hai L Van, Park HJ, Seo YB. Effect of PFI mill and Valley beater refining on
766 cellulose degree of polymerization, alpha cellulose contents, and

crystallinity of 767   wood and cotton fibers. Journal of Korea Technical Association
of the Pulp and 768   Paper Industry 2013;45:27–33.
doi:10.7584/ktappi.2013.45.4.027.

769   [48]   Besbes I, Rei M, Boufi S. Nanofibrillated cellulose from Alfa , Eucalyptus and Pine

770   fibres : Preparation , characteristics and reinforcing potential. Carbohydrate

771   Polymers 2011;86:1198–206. doi:10.1016/j.carbpol.2011.06.015.

772   [49]   Zuluaga R, Putaux J-LL, Restrepo A, Mondragon I, Gañán P. Cellulose

773   microfibrils from banana farming residues: Isolation and characterization.

774   Cellulose 2007;14:585–92. doi:10.1007/s10570-007-9118-z.

775   [50] Bhatnagar A. Processing of cellulose nanofiber-reinforced composites. Journal of

776   Reinforced Plastics and Composites 2005;24:1259–68.

777   doi:10.1177/0731684405049864.

778   [51] Börjesson M, Westman G. Crystalline Nanocellulose — Preparation, modification,779   and properties. Cellulose - Fundamental Aspects and Current Trends, InTech; 780   2015, p. 159–91. doi:10.5772/61899.

781   [52] Bondeson D, Mathew A, Oksman K. Optimization of the isolation of nanocrystals

782   from microcrystalline cellulose by acid hydrolysis. Cellulose 2006;13:171–80.

783   doi:10.1007/s10570-006-9061-4.

784   [53] Naduparambath S, T.V. J, Shaniba V, M.P. S, Balan AK, Purushothaman E.
785   Isolation and characterisation of cellulose nanocrystals from sago seed shells.786   Carbohydrate Polymers 2018;180:13–20. doi:10.1016/j.carbpol.2017.09.088.

787   [54] Ilyas RA, Sapuan SM, Ishak MR. Isolation and characterization of nanocrystalline
788   cellulose from sugar palm fibres (*Arenga Pinnata*). Carbohydrate Polymers

789   2018;181:1038–51. doi:10.1016/j.carbpol.2017.11.045.

790   [55] Lu P, Hsieh Y. Preparation and characterization of cellulose nanocrystals from

791   rice straw. Carbohydrate Polymers 2012;87:564–73.

792   doi:10.1016/j.carbpol.2011.08.022.

793   [56] Zimmermann T, Bordeanu N, Strub E. Properties of nanofibrillated cellulose from794   different raw materials and its reinforcement potential. Carbohydrate Polymers 795   2010;79:1086–93. doi:10.1016/j.carbpol.2009.10.045.

796   [57] Habibi Y, Vignon MR. Optimization of cellouronic acid synthesis by TEMPO-
797   mediated oxidation of cellulose III from sugar beet pulp. Cellulose 2008;15:177–798   85. doi:10.1007/s10570-007-9179-z.

799   [58] Yasim-Anuar TAT, Ariffin H, Norrrahim MNF, Hassan MA. Factors affecting
800   spinnability of oil palm mesocarp fiber cellulose solution for the production of801   microfiber. Bioresources 2017;12:715–34.

802   [59] Henriksson M, Berglund LA. Structure and properties of cellulose nanocomposite803   films containing melamine formaldehyde. Journal of Applied Polymer Science 804   2007;106:2817–24. doi:10.1002/app.26946.

805   [60] Ferrer A, Filpponen I, Rodríguez A, Laine J, Rojas OJ. Valorization of residual
806   empty palm fruit bunch fibers (EPFBF) by microfluidization: Production of807   nanofibrillated cellulose and EPFBF nanopaper. Bioresource Technology
808   2012;125:249–55. doi:10.1016/j.biortech.2012.08.108.

809   [61] N. E, Jane Z, K. R. Image watermarking in higher-order gradient domain.

810   advances in wavelet theory and their applications in Engineering, Physics and

811   Technology, InTech; 2012. doi:10.5772/35603.

[62]   Faix O, Lin S, Dence C. Fourier transform infrared spectroscopy. In methods in

813   lignin chemistry. Springer-Verlag 1992:83–109.

814   [63]   Alemdar A, Sain M. Isolation and characterization of nanofibers from agricultural 815   residues - Wheat straw and soy hulls. Bioresource Technology 2008;99:1664–71.816   doi:10.1016/j.biortech.2007.04.029.

817   [64]   Karimi S, Tahir PM, Karimi A, Dufresne A, Abdulkhani A. Kenaf bast cellulosic

818   fibers hierarchy: A comprehensive approach from micro to nano. Carbohydrate

819   Polymers 2014;101:878–85. doi:10.1016/j.carbpol.2013.09.106.

820   [65] Ishak MR, Sapuan SM, Leman Z, Rahman MZA, Anwar UMK. Characterization of
821   sugar palm (*Arenga Pinnata*) fibres tensile and thermal properties. Journal
of 822   Thermal Analysis and Calorimetry 2012;109:981–9. doi:10.1007/s10973-011-
823   1785-1.

824   [66] Flauzino Neto WP, Silvério HA, Dantas NO, Pasquini D. Extraction and
825   characterization of cellulose nanocrystals from agro-industrial residue – Soy hulls.
826   Industrial Crops and Products 2013;42:480–8. doi:10.1016/j.indcrop.2012.06.041.
827 [67] Yang H, Yan R, Chen H, Lee DH, Zheng C. Characteristics of hemicellulose,

828   cellulose and lignin pyrolysis. Fuel 2007;86:1781–8.

829   doi:10.1016/j.fuel.2006.12.013.

830   [68] Deepa B, Abraham E, Cherian BM, Bismarck A, Blaker JJ, Pothan LA, et al.

831   Structure, morphology and thermal characteristics of banana nano fibers obtained

832   by steam explosion. Bioresource Technology 2011;102:1988–97.

833   doi:10.1016/j.biortech.2010.09.030.

834   [69] Li R, Fei J, Cai Y, Li Y, Feng J, Yao J. Cellulose whiskers extracted from

835   mulberry : A novel biomass production. Carbohydrate Polymers 2009;76:94–9.

836   doi:10.1016/j.carbpol.2008.09.034.
837 [70]   Soares S, Camino G, Levchik S. Comparative study of the thermal decomposition
838   of pure cellulose and pulp paper. Polymer Degradation and Stability 1995;49:275–
839   83. doi:10.1016/0141-3910(95)87009-1.

840   [71] Wang Y, Wei X, Li J, Wang F, Wang Q, Kong L. Homogeneous isolation of

841   nanocellulose from cotton cellulose by high pressure homogenization. Journal of

842   Materials Science and Chemical Engineering 2013;1:49–52.

843   doi:10.4236/msce.2013.15010.
844   [72] Wang Y, Wei X, Li J, Wang F, Wang Q, Zhang Y, et al. Homogeneous isolation of
845   nanocellulose from eucalyptus pulp by high pressure homogenization. Industrial
846   Crops and Products 2017;104:237–41. doi:10.1016/j.indcrop.2017.04.032.

847

848

Fig. 1. Photographs of (a) the sugar palm tree, (b) raw sugar palm fibers, (c) bleached fibres, (d) alkali-treated fibres, and (e) refined fibres.
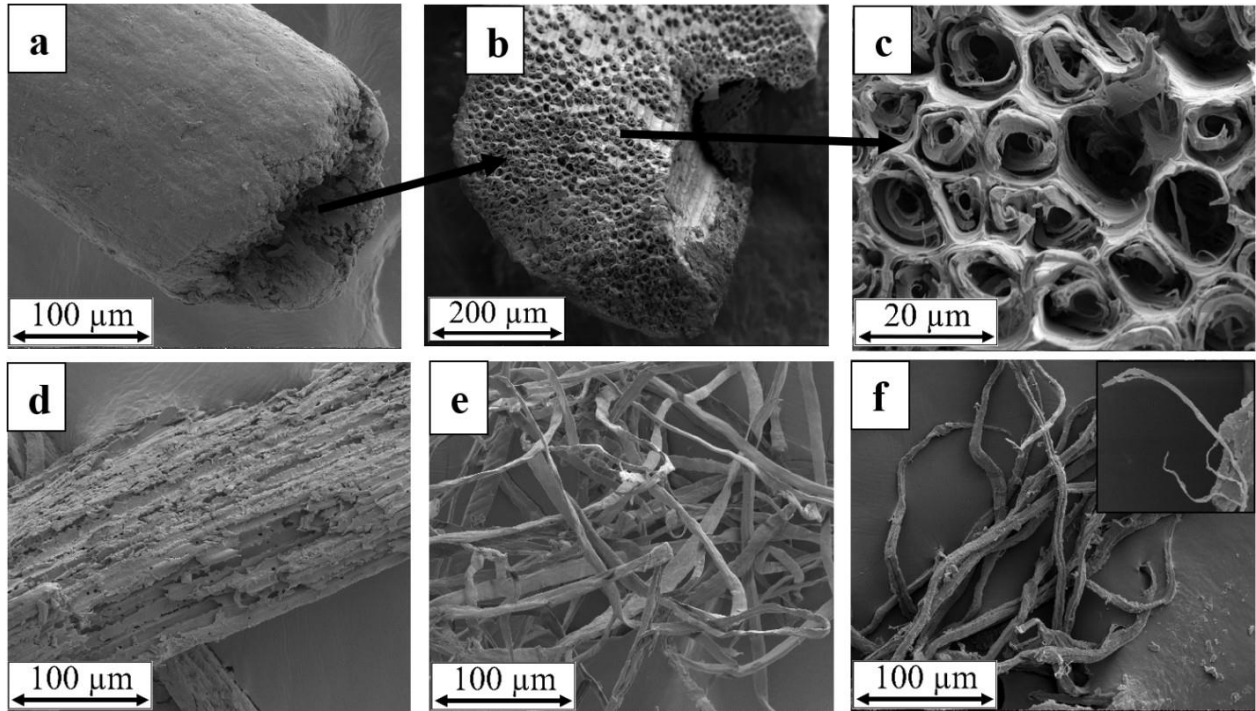
Fig. 2. FE-SEM micrographs of (a) longitudinal section of raw sugar palm fibres, (b) cross section of raw sugar palm fibres, (c) primary, secondary cell wall and middle lamella, (d) bleached fibres, (e) alkali-treated fibres, and (f) refined fibres.
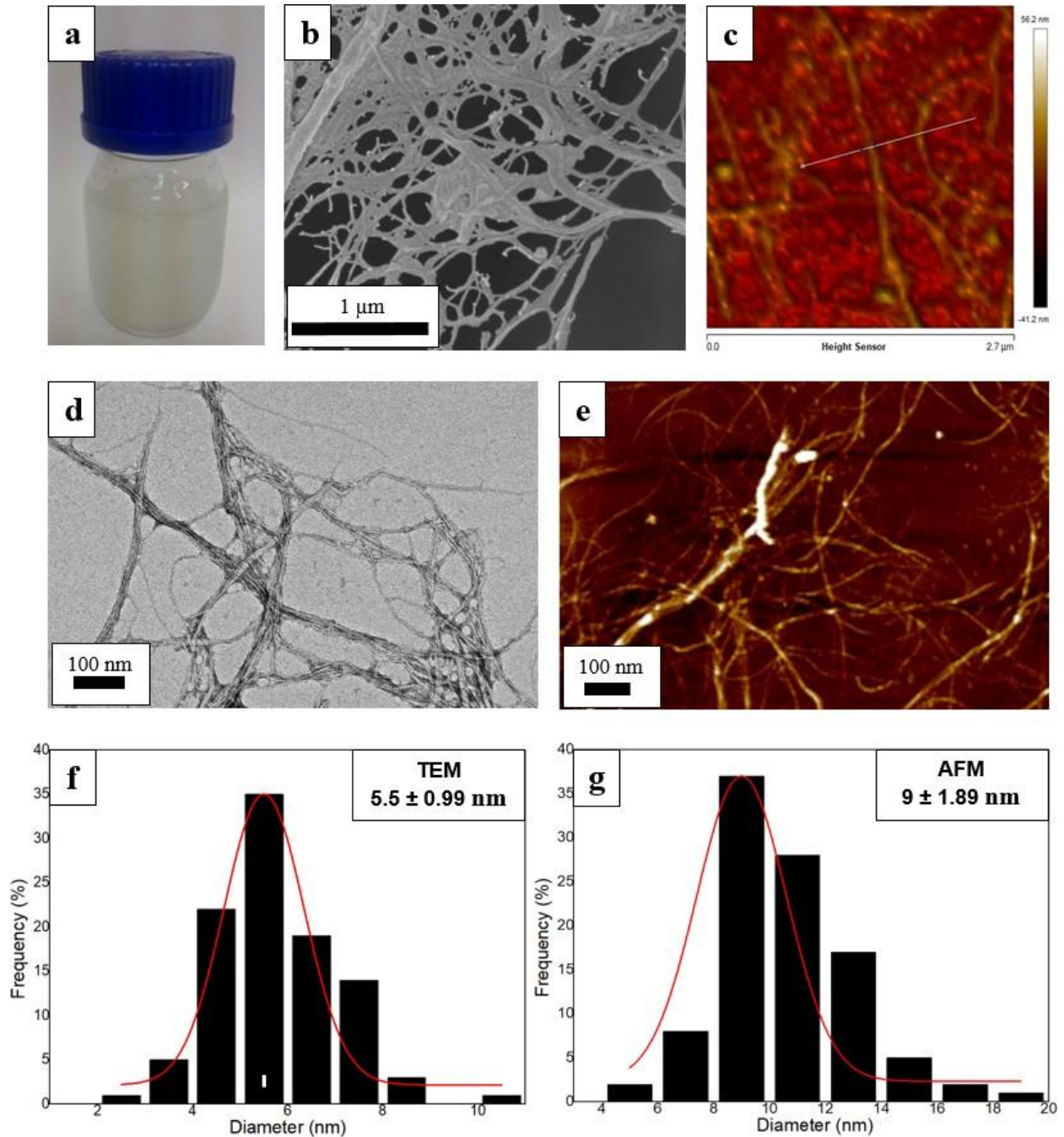
Fig. 3. (a) 2 wt% of nanocellulose suspension (b) field emission scanning electron microscopy (FESEM) micrograph, (c) height dimension of NFCs by means of atomic force microscopy (AFM) nanograph, (d) transmission electron microscopy (TEM) nanograph, (e) atomic force microscopy (AFM) nanograph, and (f and g) their diameter histograms based on TEM and AFM nanograph.
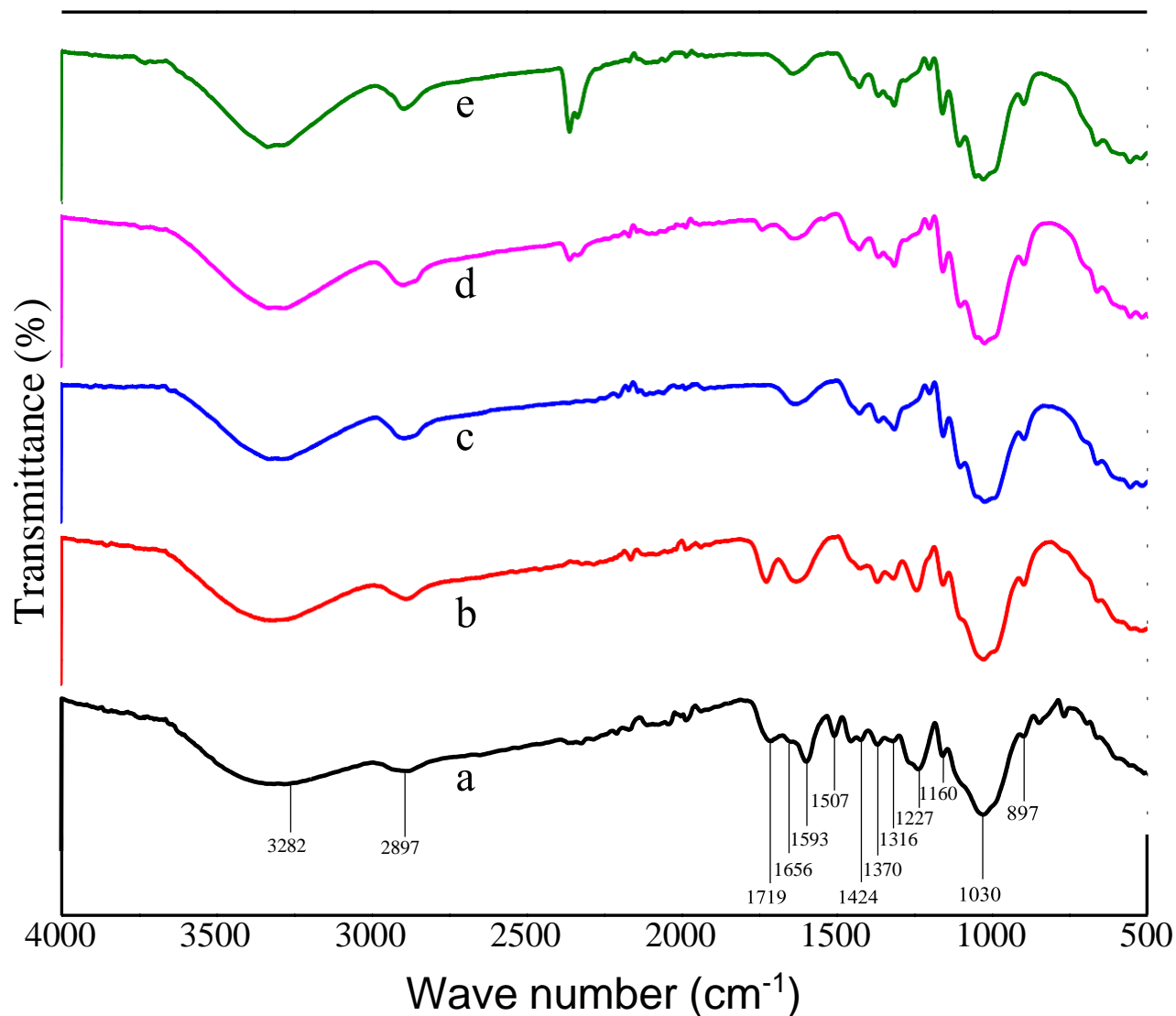
Fig. 4. Fourier-transform infrared spectroscopy of (a) raw sugar palm fibre [54], (b)bleached fibre [54], (c) alkali-treated fibre [54], (d) refined fibre, and (e) sugar palm nanofibrillated cellulose.
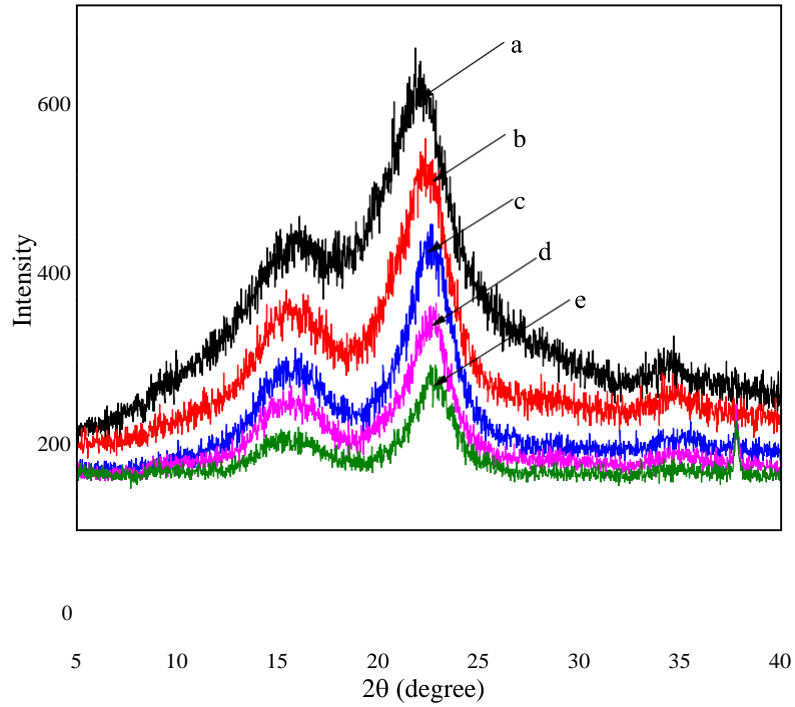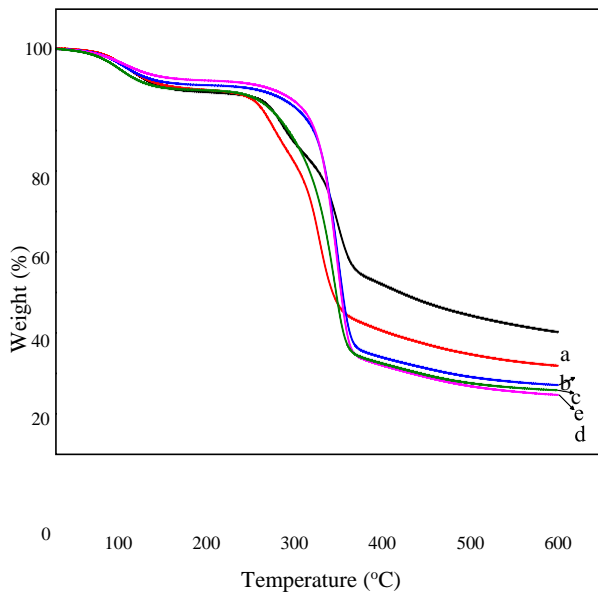
Fig. 5. XRD arrays of (a) raw sugar palm fibres [54], (b) bleached fibres [54], (c) alkali-treated fibres [54], (d) refined fibres, and (e) SPNFCs.
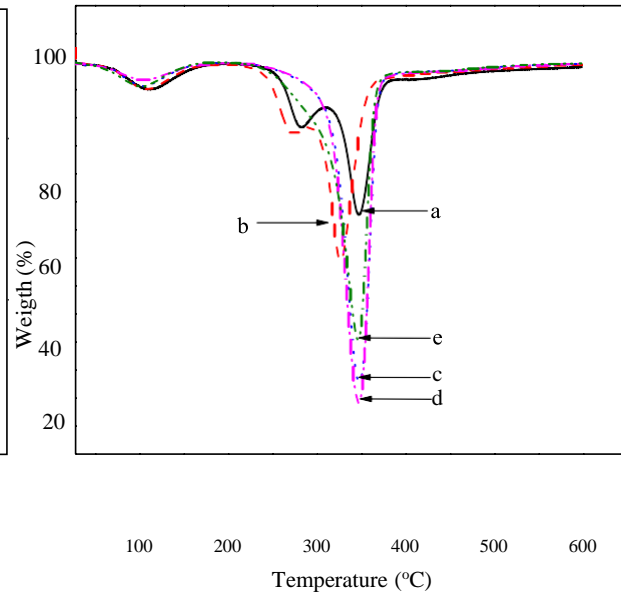
i)

ii)

Fig. 6. (i) Thermogravimetry (TG) and (ii) derivative thermogravimetric (DTG) curvesfor (a) raw sugar palm fibres [54], (b) bleached fibres [54], (c) alkali-treated fibres [54], (d) refined fibre and (e) SPNFCs.

1 **Table 1**

2 # Chemical constituent of sugar palm fibres at various stage of treatment.

Samples	Cellulose (%)	Lignin (%)	Hemicellulose (%)	Holocellulose (%)	Ash (%)	Extractive (%)
SPF	43.88	33.24	7.24	51.12	1.01	2.73
SPATF	56.67	0.27	19.8	76.47	2.16	0.3
SPC	82.33	0.06	3.97	86.3	0.72	-
SPRF	88.79	0.04	3.85	94.64	0.74	-

3 * SP = Raw sugar palm fibres; SPATF = sugar palm acid-treated fibres; SPC = sugar
4 palm alkali-treated fibres; SPRF = sugar palm refined fibres

5

6 # Table 2

7 **Table 2 Physical properties of SPF [54], SPATF [54], SPC [54], SPRF, SPNFCs, and**
8 # others nanofibres.

Samples	Diameter	Density (g/cm^{-3})	Moisture content (wt %)	X_c (%)	Surface area (m^2/g)	Pore volume (cm^3/g)	DP	M_w (g/mol)	Ref
SPF	212.01 ± 2.17 µm	1.50	3.36 ± 0.0984	55.8	7.58	0.0607	-		[54]
SPATF	94.49 ± 0.03 µm	1.30 ± 0.0023	5.25 ± 0.0745	65.9	10.35	0.0678	2963.33	480,513.39	[54]
SPC	11.87 ± 1.04 µm	1.28 ± 0.0019	3.83 ± 0.1037	76.0	13.18	0.1950	946.48	153,458.51	[54]
SPRF	3.925 ± 0.26 µm	1.26 ± 0.001	3.08 ± 0.2231	77.7	13.66	0.2010	784.76	127,251.5	Current study
SPNFCs	5.5 ± 0.99 nm	1.1 ± 0.0026	12.855 ± 0.8912	81.2	14.01	0.2109	289.79	46,989	Current study
Eucalyptus urograndis NFC	30 nm	-		82	-	-	-		[65]
Kenaf Bast Fibre NFC	1-30 nm	-	-	81.5	-	-	-	-	[66]
Pineapple Leaf NFC	30 nm	-		75.38	-	-	-		[67]
			-					-	
			-					-	

9 Results expressed as mean ± standard deviation

10

11

12

13

14

16 Table 3

17 Table 3 Decomposition temperature of SPF[54], SPATF[54], SPC[54], SPRF, and
18 SPNFCs.

Samples	Moisture evaporation			First stage decomposition			Second stage decomposition			Char yield	Ref
	T_{Onset} (◦C)	T_{Max} (◦C)	W_L (%)	T_{Onset} (◦C)	T_{Max} (◦C)	W_L (%)	T_{Onset} (◦C)	T_{Max} (◦C)	W_L (%)	W (%)	[54]
Sugar palm fibres	41.73	106.78	10.38	210.58	281	15.13	308.05	345.45	43.76	30.73	[54]
Bleached fibres	42.37	103.74	9.87	195.66	271.56	15.24	288.35	324.44	52.39	22.5	[54]
Alkali-treated fibre	43.49	101.23	8.58	207.92	346.09	73.71	-	-	-	17.71	[54]
SPPFI	33.60	104.93	7.6	204.29	345.77	76.35	-	-	-	14.86	Current study
SPNFCs	28.71	102.80	8.94	192.71	347.30	72.44	-	-	-	17.17	Current study

19

Author Agreement

Submission of work requires that the piece to be reviewed has not been previously published. Upon acceptance, the Author assigns to the Journal of Materials Research and Technology (JMRT) the right to publish and distribute the manuscript in part or inits entirety. The Author's name will always be included with the publication of the manuscript.
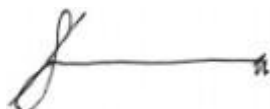
The Author has the following nonexclusive rights: (1) to use the manuscript in the Author's teaching activities; (2) to publish the manuscript, or permit its publication, aspart of any book the Author may write; (3) to include the manuscript in the Author's own personal or departmental (but not institutional) database or on-line site; and (4) tolicense reprints of the manuscript to third persons for educational photocopying. The Author also agrees to properly credit the Journal of Materials Research and Technology(JMRT) as the original place of publication.

The Author hereby grants the Journal of Materials Research and Technology (JMRT) full and exclusive rights to the manuscript, all revisions, and the full copyright. The Journal of Materials Research and Technology (JMRT) rights include but are not limited to the following:

(1) to reproduce, publish, sell, and distribute copies of the manuscript, selections of themanuscript, and translations and other derivative works based upon the manuscript, in print, audio-visual, electronic, or by any and all media now or hereafter known or devised; (2) to license reprints of the manuscript to third persons for educational photocopying; (3) to license others to create abstracts of the manuscript and to index the manuscript; (4) to license secondary publishers to reproduce the manuscript in print,microform, or any computer-readable form, including electronic on-line databases; and

(5) to license the manuscript for document delivery. These exclusive rights run the fullterm of the copyright, and all renewals and extensions thereof.

I hereby accept the terms of the above Author Agreement.

Author :- S.M. Sapuan   Date :- 30/08/2018

Editor in Chief:- Marc André Meyers   Date:-

Available online at www.sciencedirect.com

jmr&t
Journal of Materials Research and Technology
www.jmrt.com.br

ELSEVIER

jmr&t

Original Article

Sugar palm (*Arenga pinnata* (*Wurmb.*) Merr) cellulosic fibre hierarchy: a comprehensive approach from macro to nano scale

Rushdan Ahmad Ilyas [a,b,*], Salit Mohd Sapuan [a,b,c,**], Rushdan Ibrahim [d], Hairul Abral [e], M.R. Ishak [f], E.S. Zainudin [a], Mochamad Asrofi [g], Mahmud Siti Nur Atikah [h], Muhammad Roslim Muhammad Huzaifah [a], Ali Mohd Radzi [a,i], Abdul Murat Noor Azammi [b,j], Mohd Adrinata Shaharuzaman [b,k,l], Norizan Mohd Nurazzi [a,b], Edi Syafri [m], Nasmi Herlina Sari [n], Mohd Nor Faiz Norrrahim [o], Ridhwan Jumaidin [p]

[a] Laboratory of Biocomposite Technology, Institute of Tropical Forestry and Forest Products, Universiti Putra Malaysia, 43400 UPM Serdang, Selangor, Malaysia
[b] Department of Mechanical and Manufacturing Engineering, Universiti Putra Malaysia, 43400 UPM Serdang, Selangor, Malaysia
[c] Advanced Engineering Materials and Composites Research Centre, Department of Mechanical and Manufacturing Engineering, Universiti Putra Malaysia, 43400 UPM Serdang, Selangor, Malaysia
[d] Pulp and Paper Branch, Forest Research Institute Malaysia, 52109 Kepong, Selangor, Malaysia
[e] Department of Mechanical Engineering, Andalas University, 25163 Padang, Sumatera Barat, Indonesia
[f] Department of Aerospace Engineering, Universiti Putra Malaysia, 43400 UPM Serdang, Selangor, Malaysia
[g] Laboratory of Material Testing, Department of Mechanical Engineering, University of Jember, Kampus Tegalboto, Jember 68121, East Java, Indonesia
[h] Department of Chemical and Environmental Engineering, Universiti Putra Malaysia, 43400 UPM Serdang, Selangor, Malaysia
[i] Faculty of Engineering and Technology, Linton Unversity Colledge, 71700 Mantin, Negeri Sembilan, Malaysia
[j] Automotive Department, Malaysia France Institute, University Kuala Lumpur, 43650 Bandar Baru Bangi, Selangor, Malaysia